51st AIAA Aerospace Sciences Meeting including the New Horizons Forum and Aerospace Exposition
07 - 10 January 2013, Grapevine (Dallas/Ft. Worth Region), Texas

AIAA 2013-0437

Interfacial Water as a Mars ISRU Objective: Detection of microscopic water using fiber optic sensors

O.J. Igbinosun[1], S.E. Wood[2], and A.P. Bruckner[3]
University of Washington, Seattle, WA 98195

Development is underway to integrate fiber optic sensors into environmental simulations of non-terrestrial environments. These sensors will allow measurement of small volumes (~μm^3) of water and will enable characterization of the thermal properties of soils. The techniques used in this study are also beneficial in determining water/ice behavior in arid environments such as those experienced on the planet Mars. The implications of this work could impact future space missions in regard to the availability of critical resources (i.e., water) for human missions and the search for non-terrestrial life.

Nomenclature

a.u.	=	arbitrary units
d	=	diameter (mm)
d_p	=	penetration depth (nm)
DTGS	=	deuterated triglycine sulfate
FTIR	=	Fourier Transform Infrared
IRE	=	Internal Reflectance Element
n_1	=	refractive index (medium 1)
n_2	=	refractive index (medium 2)
n_{21}	=	n_2/n_1
N_2	=	Nitrogen gas
NA	=	numerical aperture
NIR	=	near-infrared
P	=	water vapor pressure (mb)
P_{sat}	=	saturated water vapor pressure (mb)
R	=	reflectance
T	=	transmittance
θ_{crit}	=	critical angle

I. Introduction

WATER on Mars is always of interest to the scientific community, but an understanding of how local resources can be utilized for human space missions needs to also be addressed. ISRU (*In-Situ* Resource Utilization) can significantly reduce the mass of consumables needed for manned space missions, thus reducing the mass (and cost) needed to launch from Earth[1-3]. Materials for life support (such as oxygen and liquid water), rocket propellants, construction materials, and thermal energy are just a few examples of potential resources that could be produced on Mars[4].

There are three dominant reservoirs of water on Mars—the polar regions, the atmosphere, and the subsurface. Each presents a unique set of challenges when considering how to provide liquid water to support a permanent human presence on Mars. Locations presumed to contain substantial amounts of subsurface ice and the polar regions are at latitudes where average temperatures are very low. Although studies have shown that extracting

[1] Graduate Student, Astrobiology Program and Department of Earth and Space Sciences.
[2] Research Assistant Professor, Department of Earth and Space Sciences.
[3] Professor, Department of Aeronautics and Astronautics. Fellow, AIAA.

atmospheric water vapor via zeolite molecular sieve adsorption at Mars conditions is feasible[5,6], the amount of water acquired from the atmosphere may not be sufficient to support human missions, due to the paucity of available atmospheric water (global annual average ~10 precipitable micrometers[7]). However, interfacial water, i.e., water that exists at interfaces (e.g., thin liquid films present at the interface between mineral grains and ice or at the interface of a surface and the atmosphere) could pose a significant source for extracting consumable water. Spectral data suggest that minerals, such as zeolites, are present on the surface of Mars[8]. Zeolites exhibit a micro-porous structure, providing significant surface area for water adsorption[9]. Water equivalent hydrogen (WEH) values, obtained from the neutron spectrometer aboard the Mars Odyssey spacecraft indicated 2-10 wt.% water in the upper meter of regolith in some equatorial regions[10]. However, the availability of this water and its extractability are unknown.

Several authors have experimentally investigated the abundance of water in Mars analog soils under a variety of conditions[11,12]. Current methods of water detection in soils rely on gravimetric, conductivity, or gas chromatographic measurements[11,12]. While these methods are reliable, the advantage of using optical sensors provides the ability to carry out localized measurements *in-situ*, without having to alter or displace samples. This work is not intended to replace current methods, rather the strength of the technique presented in this paper lies in its ability to supplement and enhance the fidelity of current methods by providing real-time sensing of microscopic water in dynamic, non-uniform environments.

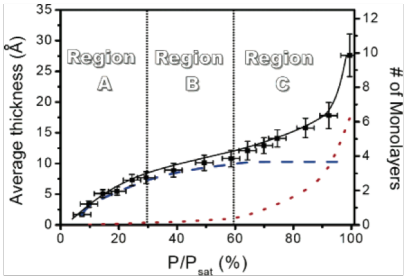

Figure 1. Adsorption isotherm of water adsorbed to a silicon surface. The number of monolayers of adsorbed water is plotted as a function of relative humidity (P/P_{sat}). Regions A, B, and C indicate the evolution of the nature of the layers (A: ice-like, B: transitional, C: liquid-like) [13].

Studies have shown that interfacial water may be as mobile as liquid water[13] and that terrestrial microbes are capable of utilizing these thin films for metabolic processes[14,15]. Adsorption isotherms of silicon oxide as a function of relative humidity have been investigated by Asay and Kim.[13] using a similar technique to that described in this paper. Figure 1 shows the results of that work, which indicate a BET Type II behavior, implying strong physical adsorption followed by multilayer adsorption. Their work also described the correlation between the asymmetric/stretching O-H vibrations to the mobility of water molecules in adsorption layers. Regions where the asymmetric stretch dominated indicates more mobile, "liquid-like" layers, whereas, symmetric-stretch-dominated layers indicate less mobile, more structurally bound "ice-like" layers. These "liquid-like" layers could provide mobile water to microbial life[14, 15].

II. Experimental Technique

Internal Reflection Spectroscopy refers to a sampling technique that utilizes the evanescent field (created at an interface where total internal reflection occurs) used in conjunction with spectroscopy. Total internal reflection occurs when light propagating from a medium with a higher index of refraction meets the interface of a medium with a lower refractive index at angles greater than the critical angle, θ_{crit} (Fig. 2a). The critical angle is defined as the angle of incidence for which the angle of refraction is 90° (Eq. (1)), derived from Snell's law, and is determined by the refractive indices of the media involved[15]. In this equation n_1 is the originating medium and n_2 is the refracted

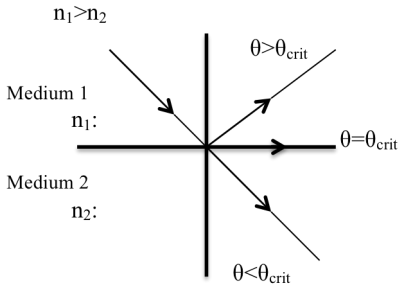

Figure 2. Evanescent field of internally reflected light. (a) This phenomenon occurs at angles (θ) greater than the critical angle (θ_{crit}). (b) Molecules within the evanescent field preferentially absorb light, which allows them to be characterized during analysis.

medium.

$$\theta_{crit} = sin^{-1}\, n_2/n_1, \tag{1}$$

Although light is reflected at the interface between two media, a fraction of the light (known as the evanescent field) penetrates from the originating medium to the other. The distance the electric field of the light wave penetrates into the second medium is called the penetration depth, d_p, and is a function of wavelength, refractive index, and incidence angle (Eq. 2). The penetration depth is defined as the distance required for the amplitude of the electric field to fall to $1/e$ of its value at the surface[16].

$$d_p = \lambda\left[2\pi n_1\sqrt{\left(\sin^2\theta - n_{21}^2\right)}\right]^{-1} \tag{2}$$

The penetration depth is an important component of this work because it allows determination of the maximum extent of the electric field, which provides a framework for spectral analysis of the media within the field. In the present work an optical fiber was used to introduce the evanescent field into the medium of interest (humid air, water, or analog planetary soils) (Fig. 2b). The light source used in the present study was broadband; thus, the penetration depth varied as a function of wavelength, as well as with incidence angle, and for the types of optical fibers used. The type of fiber used in this study was a step-index multimode optical fiber. As the name suggests several modes (at varying wavelengths) can exist as light propagates within the optical fiber. Due to the broadband light source and other design components, the incidence angle also varied. However, the variation was limited by the numerical aperture, NA, of the optical cable and θ_{crit}, and was calculated so that the penetration depth could be averaged at the wavelengths used in this study.

Water has absorption bands in both the near-infrared and the infrared[17, 18]. The near-infrared region (NIR) (1-2.5 μm) contains several overtone and combination absorptions bands, which allow detection and quantification of small volumes of water. NIR transmitting optical fibers could be more easily acquired, and at less expense than those capable of transmitting at longer wavelengths; accordingly, NIR-transmitting fibers were used in the study.

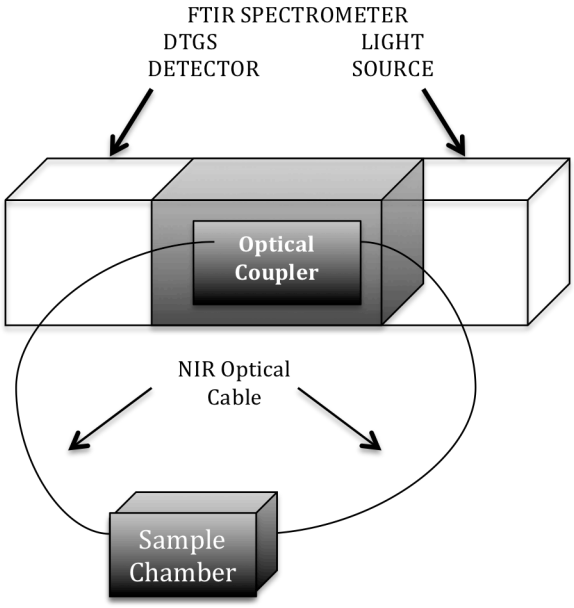

Figure 3. Facility setup. Sample chamber and NIR optical cable.

III. Experimental Facility

The experimental facility (Fig. 3) used in this work included a Vector 33 Fourier Transform Infrared (FTIR) Spectrometer, a Harrick Scientific Fibermate 2 fiber optic coupler, NIR optical cables, and a sample chamber. The spectrometer is equipped with a deuterated triglycine sulfate (DTGS, a common component used in detectors for infrared spectroscopy) detector and light sources which transmit in the near-infrared and infrared (1.2-20 μm). Spectra were acquired by coupling a fiber optic cable to the spectrometer via the optical coupler.

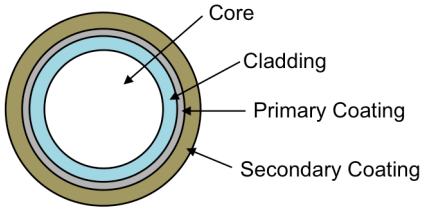

Figure 4. Cross-section of typical fiber optic cable.

Most optical fibers (Fig. 4) have several layers surrounding the core[19]. These layers provide both optical and mechanical functions. The first layer, or cladding, is

typically a material with a lower refractive index than the core (allowing for total internal reflection), and is typically either a polymer or glass. The next layer (primary coating), commonly referred to as a buffer, provides protection and flexibility to the cable. Lastly, a secondary coating or jacket and other insulating materials form the thickest layer to protect the fiber. The full assembly is referred to as the optical cable. To enable sensing, the optical cable was modified by chemically stripping a small section (~5 cm) to expose the core, which is henceforth referred to as the internal reflectance element (IRE). The IRE was housed in the sample chamber (Fig. 5) where all measurements were performed. The fiber optic cable used in this study had a core diameter of 1000 μm, transmission capability

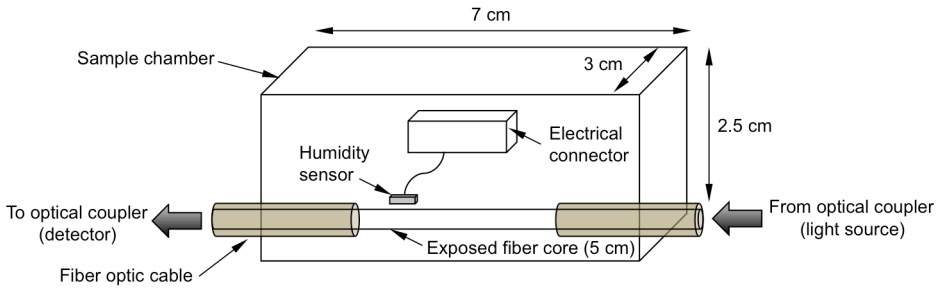

Figure 5. Sample Chamber

within the NIR at the water absorption bands of interest, and was obtained from Thorlabs.

The use of the fiber-optic coupler and the optical fiber itself both contribute to a decrease in the amount of light reaching the detector. Rather than passing freely through the length of the sample compartment, light enters the coupler, reflects off a series of mirrors (within the coupler) and exits via a SMA connection (Fig 3). Once an optical fiber is attached to the coupler, light enters and propagates within the length of the cable and re-enters the coupler at another SMA connection. Once again, light is reflected via a series of mirrors, exits the coupler, and enters the detector. To minimize the loss in the fiber, its length was chosen to be just long enough to connect the coupler to the sample chamber and back to the coupler (2.0 m).

IV. Results and Future Work

Wavelengths of 5260 cm^{-1} (~1900 nm) and 7140 cm^{-1} (~1400 nm), corresponding to NIR absorptions bands of water, were used in the experiments. Since the 5260 cm^{-1}absorption band is much stronger (Fig. 6), it was the primary one used for our analysis. The vertical axis is the log of the inverse transmittance, *1/T*. Absorption of light by water within the evanescent field is shown here as peaks at 5260 cm^{-1} and 7140 cm^{-1}. Figure 6 shows absorption by water increasing as the IRE is slowly immersed in water. To accomplish this, the sample chamber was oriented vertically and slowly filled with water. A transmission spectrum was taken at each coverage increment and was normalized to reference spectra taken under dry conditions (relative humidity ~0.1). The depths of the absorptions are converted and plotted with respect to IRE coverage in Fig. 7. Figure 8 shows the absorption of water adsorbed on the IRE as a function of relative humidity (P/P_{sat}). Transmission spectra were acquired at a range of relative humidities (8.1-96%), at room temperature (~22°C). A Sensirion capacitive relative humidity sensor was placed in close proximity to the IRE within the sample chamber (Fig. 5) to detect changes in vapor pressure, *P*. The sample chamber was purged with

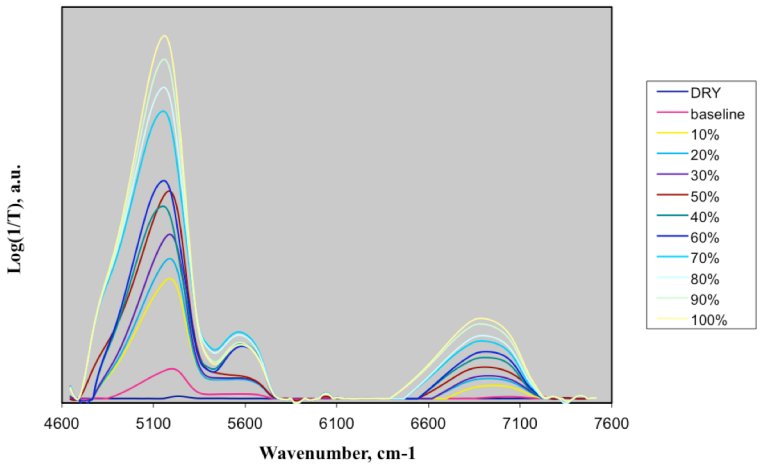

Figure 6. Near infrared spectra showing increased absorption as a function of increasing surface area coverage of IRE.

dry nitrogen prior to reference spectra being taken. The humidity was controlled by adding small amounts of liquid water to the sample chamber and monitoring increases in relative humidity. Once conditions stabilized, a transmission spectrum was taken. This process was repeated to provide a range humidity-specific spectra. Again, spectral absorption was found to increase with increasing water content (i.e., relative humidity). Increasing vapor pressure correlates to an increasing concentration of water molecules on the surface of the IRE as adsorption layers (adlayers) build. At high humidites there can be as many as ten adlayers present on the surface of the IRE (each layer having a depth of a single water molecule)[13]. Increased absorption with relative humidity, as shown in Fig. 8, is consistent with the liquid water absorption data in Fig. 7, in that the spectral absorption of liquid water is greater than absorption occurring when only adsorbed water is present (relative humidity < 100%).·

In order to estimate unknown volumes of water within the penetration depth of the IRE, a relationship between volume and spectral absorption is required. When the IRE is completely immersed in liquid water, a maximum spectral absorption is reached and can be associated with a penetration depth of the evanescent wave. Equation 2 was used to calculate penetration depths at 5260 cm^{-1}. Assuming water within the evanescent field fills uniformly, the volume can be approximated to a cylindrical shell whose thickness is equal to d_p. The measured absorptions in Fig. 8 are also dependent on the penetration depth, so these absorptions can be linked to volume approximations. Table 1 displays estimates of volume as a function of IRE coverage within the penetration depth for a 5-cm IRE. Therefore, the curves in Fig. 6 can be used to estimate the volume of an unknown substance (e.g., ice, liquid water) within the evanescent field, based on spectral absorption and IRE coverage. For example, if spectral absorption at 5260 cm^{-1} corresponds to the red curve in Fig. 6 (50% coverage of the IRE), then ~.466 mm^3 of water is within the evanescent field.

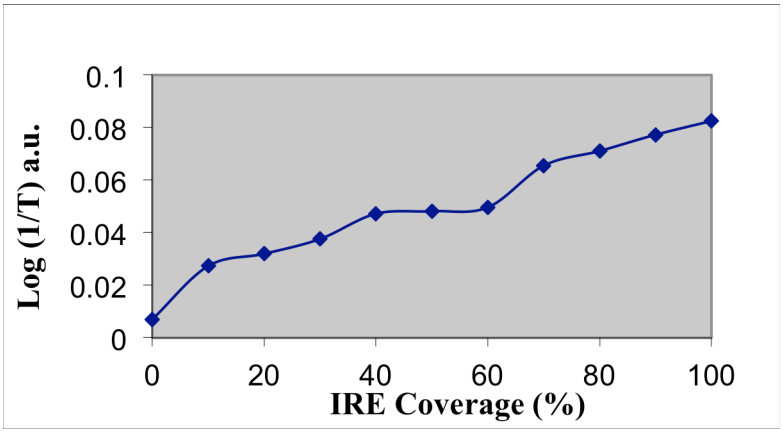

Figure 7. Water absorption with respect to changes in liquid water at 5260 cm^{-1}.

The NIR IRE mentioned in this work is one of two sensors that will be developed and incorporated into a calibration chamber capable of measuring thermal data on Mars analog soils at Mars environmental conditions. The other sensor will be constructed from chalcogenide glass, capable of transmitting light from 2-7 µm. Combined, these sensors will be used to observe changes in water absorption bands indicative of changes in the structure of adsorbed layers and the presence of water. Data collected from these experiments will be used to model adsorption water layer structure relative to water vapor partial pressure in Mars analog soils on diurnal and seasonal time scales, to identify liquid-like layers that could persist on the surface of mineral grains within the Mars regolith. In addition, the quantification of adlayers and the rates of sorption/desorption will supply critical information about the amount of water present in soils for extraction purposes in ISRU systems and have

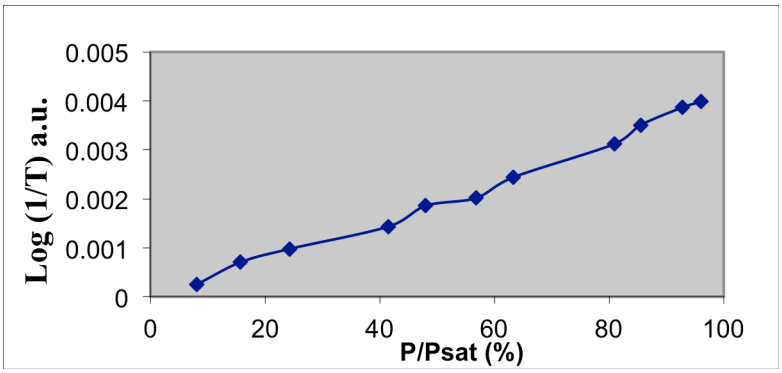

Figure 8. Water absorption with respect to changes in relative humidity at 5260 cm^{-1}.

· Note the difference between the words "adsorbed" and "absorbed."

astrobiological implications.

Table 1. Estimated Volume as a function of IRE Coverage for a 5 cm IRE (d = 1 mm).

IRE Coverage (%)	Volume within d_p at 5260 cm^{-1} [$*10^{-1}$ mm^3]
10	0.93
20	1.86
30	2.80
40	3.73
50	4.66
60	5.59
70	6.53
80	7.46
90	8.39
100	9.32

Acknowledgments

O. J. Igbinosun wishes to thank E. Abramson, M. McCarthy, R. Holzworth, and A. Gillespie in the Dept. of Earth & Space Sciences at the University of Washington for their advice and assistance, and to A. Hart in the Dept. of Atmospheric Sciences and L. Kruse in the Dept. of Chemistry for their assistance with the experiment. This material is based upon work supported by the National Science Foundation Graduate Research Fellowship, under Grant No. DGE-0718124.

References

[1]Ash, R. L., Dowler, W. L., and Varsi, G., "Feasibility of Rocket Propellant Production on Mars," *Acta Astronautica* **5**, 705-724, 1978.

[2]Zubrin, R. M., "In-Situ Propellant Production: The Key Technology Required for the Realization of a Coherent and Cost-Effective Space Exploration Initiative," AIAA-91-668, 42nd Congress of the International Astronautical Federation, Montreal, Canada, October 1991.

[3]Grover, M. R., and Bruckner, A. P., "Water Vapor Extraction from the Martian Atmosphere by Adsorption in Molecular Sieves," Paper AIAA 98-3302, 34th AIAA/ASME/SAE/ASEE Joint Propulsion Conference, Cleveland, OH, July 1998.

[4]Sanders, G. B. and Duke, M., *NASA In-Situ Resource Utilization (ISRU) Capability Roadmap Executive Summary*, International Lunar Conference on the Exploration and Utilization of the Moon, Toronto, Canada, Sept. 18-23, 2005. http://sci2.esa.int/Conferences/ILC2005/Manuscripts/SandersG-02-DOC.pdf

[5]Schneider, M. "Experimental Investigation of Water Vapor Adsorption by Molecular Sieve Zeolite 3A under Simulated Martian Atmospheric Conditions," MS thesis, Department of Aeronautics & Astronautics, University of Washington, Seattle, WA, 2003.

[6]Schneider, M. A., and Bruckner, A. P., "Extraction of Water from the Martian Atmosphere," *Space Technology & Applications International Forum – STAIF-2003*, Albuquerque, NM, Feb. 2-5, 2003, M.S. El-Genk, ed., American Institute of Physics Conference Proceedings, Volume 654, pp. 1124-1132.

[7]Smith, M. D., "The annual cycle of water vapor on Mars as observed by the Thermal Emission Spectrometer," *J. Geophys. Res.*, **107** (E11), 5115, doi:10.1029/2001JE001522, 2002.

[8]Ruff, S. W., "Spectral Evidence for zeolite in the dust on Mars," *Icarus*, **168**, 131-143, 2004.

[9]Gregg, S. J., and Sing, K. S. W., *Adsorption, Surface Area and Porosity*, Academic Press, London, 1982.

[10]Feldman, W. C., *et al.* "Global Distribution of Near-Surface Hydrogen on Mars," *J. Geophys. Res.*, **109**, E09006, doi:10.1029/2003JE002160, 2004.

[11]Janchen *et al.*, "Investigation of the water sorption properties of Mars-relevant micro- and mesoporous minerals," Icarus, **108**, 353-358, 2006.

[12]Hudson, T. L., Aharonson, O., Schorghofer, N., "Laboratory experiments and models of diffusive emplacement of ground ice on Mars," *J. Geophys. Res.*, **114**, e01002, doi:10.1029/2008JE003149, 2009.

[13]Asay, D. B., and Kim, S. H., "Evolution of the Adsorbed Water Layer Structure on Silicon Oxide at Room Temperature," *J. Phys. Chem.*, **109**, 16760-16763, 2005.

[14]Rivkina, E. M. "Metabolic Activity of Permafrost bacteria below the freezing point," *Applied and Environmental Microbiology*, **8**, 3230-3233, 2000.

[15]Ostroumov, V. E., and Siegert, C., "Exobiological aspects of mass transfer in microzones of permafrost deposits. *Advances in Space Research*, **12**, 79-86, 1996.
[16]Harrick, N. J., *Internal Reflection Spectroscopy*, Interscience Publishers, New York, 1967, Chaps. 2-4.
[17]Curcio, J. A., and Petty, C.C., "The Near Infrared Absorption Spectrum of Liquid Water," *Journal of the Optical Society of America,* 41,302-304, 1951.
[18]Hale, G. M., and Querry, M. R., "Optical constants of water in the 200-nm to 200-µm wavelength region," *Applied Optics*, **12**, 555-563, 1973.
[19]Thyagarajan, K., Ghatak, A., *Fiber Optic Essentials*, John Wiley & Sons Inc, New Jersey, 2007, Chap. 4.